

ADSORBED FUNCTIONALIZED PORPHYRINS ON POLYANILINE MODIFIED PLATINUM ELECTRODES. COMPARATIVE ELECTROCHEMICAL PROPERTIES

B.O. TARANU^a, E. FAGADAR-COSMA^{b*}, I. POPA^a, N. PLESU^b, I. TARANU^a
^a*National Institute for Research and Development in Electrochemistry and Condensed Matter, Aurel Paunescu Podeanu Street 144, 300860-Timisoara, Romania*
^b*Institute of Chemistry Timisoara of Romanian Academy, 24 M. Viteazu Ave, 300223-Timisoara, Romania*

Polyaniline (PANI) modified platinum electrodes with and without 5-(4-pyridyl)-10,15,20-tris(phenoxy-phenyl)porphyrin (P1) and 5,10,15,20-tetra(allyloxy-phenyl)porphyrin (P2) adsorbed on their surface were investigated comparatively. Pt electrodes were modified using electrogenerated PANI from 0.5M H₂SO₄ solutions containing aniline monomer. P1 and P2 were adsorbed on the surface of the PANI modified electrodes by consecutive immersion in benzonitrile solutions, to achieve uniform porphyrin deposition and to prevent aggregation phenomena. The electrochemical behavior of the three types of modified electrodes (PANI, PANI-P1 and PANI-P2) was studied using cyclic voltammetry in monomer free H₂SO₄ solutions. UV-Vis spectra of solubilized films were also recorded and compared. The modified electrodes were investigated as sensing materials for cation potentiometric detection in several aqueous test solutions.

(Received April 12, 2014; Accepted May 13, 2014)

Keywords: Porphyrins, Polyaniline, Cyclic voltammetry, UV-Vis absorption, Sensing materials

1. Introduction

Polyaniline (PANI) is a conducting electroactive polymer that can be easily deposited from aqueous acidic solutions containing aniline monomer [1]. Its simple synthesis method together with its potential range of applications has made PANI the subject of intensive chemical, electrochemical and optical research studies [2].

PANI can be generated by the electropolymerization of aniline using electrochemical methods such as chronopotentiometry and cyclic voltammetry, that several advantages [3,4].

The advantages of generating PANI films using cyclic voltammetry lead to a decrease in the amount of hydrolysis products incorporated in the PANI film layers and the formation of a thicker and more conductive film [5]. PANI is an environmentally stable polymer with good conductivity [6] and it has been used to design and develop solid contact potentiometric sensors, known for their simple design, short response time and for being promising candidates for automation [7].

Porphyrins are macrocyclic compounds, some of which exist naturally and others are obtained synthetically. They are extended aromatic systems and present amphoteric properties.

Porphyrins can be peripherally functionalized with a large number of substituents and the inner size of their macrocycle allows the binding of most metal ions [8]. Molecules substituted with different types and numbers of moieties show radically different properties, a characteristic that allows porphyrins to be promising candidates for a large number of applications, including:

*Corresponding author: efagadar@yahoo.com

reaction catalysts [9,10], photosensitizers in the photodynamic therapy of cancer [11] and in dye-sensitized photovoltaic cells [12,13], metal corrosion inhibitors [14], indicators in diagnosing various metabolic disorders and xenobiotic exposures [15], sensing elements [16,17] etc. Moreover, molecular electronics are based on self-assembling and self-organization and in this respect, porphyrins are recommended for film deposition [18] on different surfaces using versatile techniques [19]. Based on their tailored amphiphilic properties, porphyrins might grow and produce self-assembled nanoparticles and their structure can influence the size and shape of these nanoparticles [20], finally arranging them into highly organized architectures [21].

Lvova et. al [22] reported the development of a series of potentiometric sensors with carbonate-selective properties. The sensors were obtained using PVC polymeric membranes doped with Co(II) or Cu(II) 5,10,15-tris(4-aminophenyl)-20-phenyl porphyrins or by electrogenerating films on Pt working electrodes from solutions containing the same porphyrins and in some cases aniline as well. Potentiometric studies were performed in solutions of several salts with concentrations in the $10^{-7} \div 10^{-1}$ M range. The potentiometric responses of electropolymerized PANI films doped with Co(II) and Cu(II) porphyrins in solutions containing CO_3^{2-} anions showed slopes of 27 and 28 mV/decade, respectively. The sensors were also effective at measuring the carbonate content of human blood plasma.

The present paper describes a comparative study between PANI modified platinum electrodes with and without 5-(4-pyridyl)-10,15,20-tris(phenoxy-phenyl)porphyrin (P1) and 5,10,15,20-tetra(allyloxy-phenyl)porphyrin (P2) adsorbed on their surface. PANI was generated electrochemically using cyclic voltammetry and became substrate for porphyrin adsorption realized by immersing the PANI modified electrodes in porphyrin solutions with the final aim of developing cation sensing materials.

2. Experimental

Reagents

5-(4-pyridyl)-10,15,20-tris(phenoxy-phenyl)porphyrin (P1) and 5,10,15,20-tetra(allyloxy-phenyl)porphyrin (P2) powders were synthesized in fair yields using previously reported procedures [23,24].

P1 was synthesized by a multicomponent reaction [23] by refluxing pyridincarbaldehyde/4-phenoxybenzaldehyde/pyrrole in a molar ratio: 1/3/4, all reagents being dissolved in propionic acid as solvent. After 4 hours, the reaction was completed and the reaction mixture was cooled to room temperature and a mixture of six porphyrin derivatives were precipitated with *n*-hexane. Porphyrins containing mixed substituents and symmetrical ones were directly obtained in their oxidized form by atmospheric O_2 and further separated by column chromatography. The 5(4-pyridyl)-10,15,20-tris(4-phenoxy-phenyl) porphyrin derivative was eluted from the crude product with a mixture of 1% triethylamine (Et_3N), 3% methanol in CHCl_3 , over silica gel. Evaporation of the solvent mixture gave the violet powder solid which was recrystallised from dichloromethane.

P2 was obtained by adapted Lindsey method by condensation of pyrrole with 4-allyloxybenzaldehyde in CH_2Cl_2 under argon, at room temperature using $\text{BF}_3/\text{etherate}$ as a catalyst. Oxidation of the porphyrinogen intermediates was realized with *p*-chloranil. Flash chromatography and purification on silica gel provided the P2 porphyrin. [25,26].

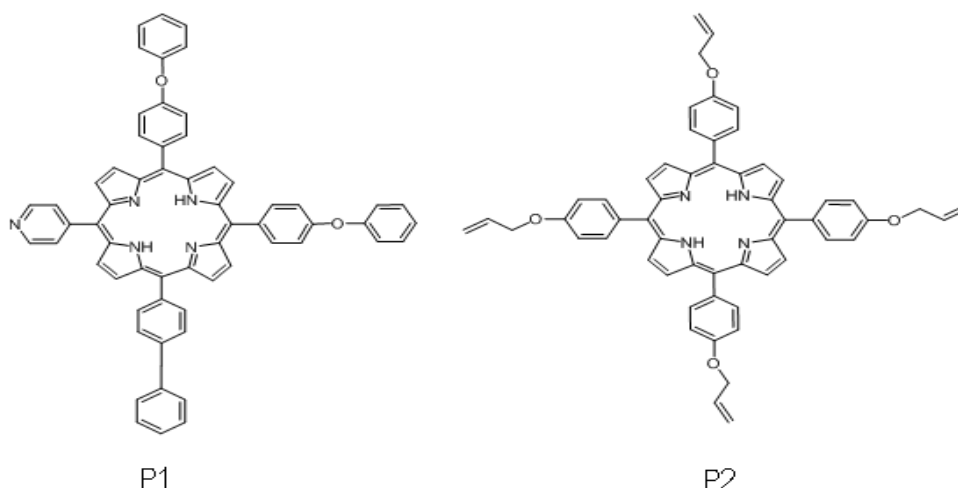


Fig. 1. Chemical structures of 5-(4-pyridyl)-10,15,20-tris(phenoxy-phenyl)porphyrin (P1) and 5,10,15,20-tetra(allyloxy-phenyl)porphyrin (P2).

Benzonitrile, N,N-dimethylformamide (DMF), H₂SO₄ (98 % purity) and aniline were purchased from Merck and all metal nitrates used in potentiometric measurements were purchased from Sigma-Aldrich. All aqueous solutions were prepared using double distilled water. Polyaniline electropolymerization experiments were performed using freshly distilled aniline.

Cyclic voltammetry studies

Cyclic voltammetry experiments were performed at room temperature using a PGZ 301 Dynamic-EIS Voltammetry potentiostat with VoltaMaster 4 software and a three-electrode electrochemical glass cell. The working electrode was the platinum plate electrode ($S = 0.45 \text{ cm}^2$) modified with PANI film with or without P1 or P2 adsorbed on its surface. The counter electrode was an unmodified platinum plate electrode ($S = 0.8 \text{ cm}^2$) and the Ag/AgCl/KCl sat. electrode was used as reference. All potentials are referenced to the HSE.

Before each deposition experiment the Pt working electrode was cleaned both chemically and electrochemically. The chemical cleaning consisted in the immersion of the electrode in chromic – sulfuric acid solution under stirring conditions for 2 minutes, followed by washing with double distilled water. The electrochemical treatment consisted in maintaining the electrode at a constant potential of 2.1 V for 5 minutes. Aniline electropolymerization was carried out by sweeping the potential between -0.2 and 1.2 V for 3 cycles, followed by a second potential cycling in the $-0.2 \div 0.85 \text{ V}$ range (20 cycles), at a scan rate $\nu = 0.05 \text{ V/s}$.

PANI was deposited from an aqueous electrolyte solution of 0.1 M aniline in 0.5 M H₂SO₄. The PANI modified electrode was immersed 2 minutes under stirring in 0.5 M H₂SO₄ aqueous solution in order to remove any unreacted aniline from its surface, was washed with double distilled water and dried at room temperature.

For porphyrin adsorption, the dried PANI modified electrode was immersed three times into a vial with benzonitrile solution containing and 1 mM P1 or P2. Each immersion lasted 1 minute and was followed by a drying stage at room temperature.

The electrochemical behavior of the three types of modified Pt electrodes (PANI, PANI-P1 and PANI-P2 electrodes), was investigated by cyclic voltammetry in 0.1 and 0.5 M H₂SO₄ aqueous solutions.

Potentiometric measurements

The ion detection performance of the PANI, PANI-P1 and PANI-P2 electrodes was investigated by potentiometric measurements, in standard solutions containing different metal cations in the concentration range $10^{-5} \div 10^{-1} \text{ M}$. The standard solutions were prepared by the successive dilution of stock solutions (0.1 M) obtained after dissolving metal nitrates (cations: Ag⁺, Cu²⁺, Cr³⁺, Ca²⁺, Co²⁺, Na⁺, Al³⁺, Mg²⁺, Zn²⁺, Cd²⁺, Pb²⁺, Sr²⁺, Ba²⁺, Ni²⁺, K⁺) in double distilled water.

The measurements were carried out at room temperature using a Hanna Instruments HI2216 pH/mV-meter and the following electrochemical cell: Ag|AgCl|KNO₃ (1M)|sample|working electrode. Before performing the measurements for each cation, the sensors were conditioned for 30 minutes by immersion in the 10⁻⁵ M solution (under stirring) of the appropriate cation.

Spectroscopic investigation

UV-Visible spectra of the PANI films with and without porphyrins adsorbed on their surface were recorded using a V530 ABLE-JASCO spectrometer, after the films were dissolved in DMF.

3. Results and discussion

Preparation of PANI, PANI-P1 and PANI-P2 modified electrodes

The PANI modified electrode was obtained through aniline electropolymerization from sulfuric acid solution, in two steps (Figure 2): in the first step, 3 cycles were recorded in the -0.2 ÷ 1.2 V potential range in order to initiate PANI synthesis [27] and in the second step, 20 cycles were recorded in the -0.2 ÷ 0.85 V range in order to avoid overoxidation reactions of the polymer chain [28]. Initial confirmation of PANI film electrogeneration on the surface of the working electrode was provided by the green color of the electrode surface.

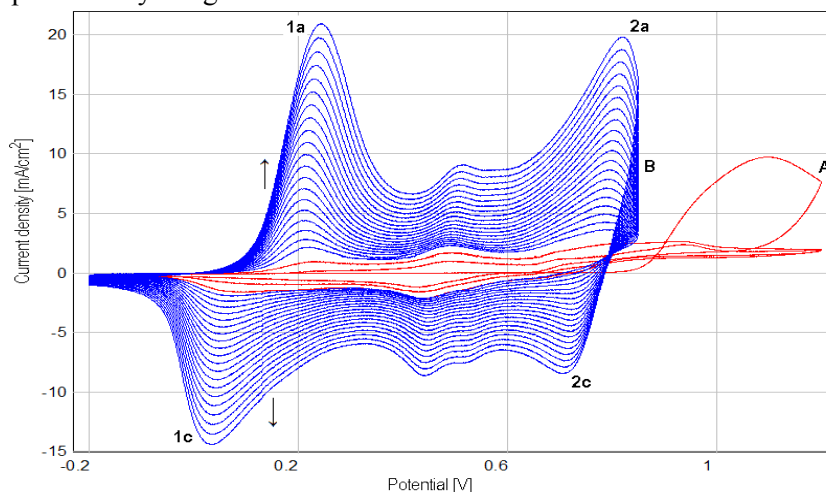


Fig. 2. Cyclic voltammograms recorded at $\nu = 0.05 \text{ V s}^{-1}$ during PANI electrogeneration on Pt electrode from aqueous solution of 0.1 M aniline in 0.5 M H₂SO₄. (A) - initiation of PANI film electrodeposition, potential range: -0.2 ÷ 1.2 V, 3 cycles; (B) - subsequent PANI film deposition, potential range: -0.2 ÷ 0.85 V, 20 cycles

The presence of the anodic peak at 1.1 V on the first cycle is due to aniline oxidation and is necessary for initiating the electrosynthesis of the polymeric film. After decreasing the potential range the film continues to grow, as shown by a steady increase in anodic and cathodic peak intensities. The presence of two reversible redox processes (**1a-1c** and **2a-2c**) and two less defined redox processes between them can be noticed. The electrochemical parameters of these redox **1a-1c** and **2a-2c** couples are shown in Table 1.

Table 1. Potential and current density values of peaks corresponding to redox couples observed during the final potential sweep of the PANI electrogeneration process.

PANI modified electrode, cycle 23	Anodic peaks			
	1a		2a	
	E(V)	i(mA/cm ²)	E(V)	i(mA/cm ²)
	0.245	20.88	0.820	19.77
	Cathodic peaks			
	1c		2c	
E(V)	i(mA/cm ²)	E(V)	i(mA/cm ²)	
0.033	-14.40	0.708	-8.44	

The anodic peak of the **1a-1c** reversible process can be attributed to the transition from the leucoemeraldine base oxidation state of PANI to the emeraldine salt oxidation state, while the cathodic peak is attributable to the reverse reaction. The two smaller peak pairs corresponding to two other redox processes are associated with the formation of intermediary compounds or secondary products during the PANI electropolymerization process, for example hydrolysis products like benzoquinone and hydroquinone [29]. The **2a-2c** redox couple corresponds to the interchanging between the emeraldine salt oxidation state of PANI and the fully oxidized pernigraniline state [30].

PANI-P1 and PANI-P2 modified electrodes were obtained by immersing the PANI modified electrode in benzonitrile solution with 0.1 M TBAP and 1mM P1 or P2, following to the procedure specified at the experimental section.

UV-Vis absorption spectra

Figures 3, 4a and 5a depict the UV-Vis absorption spectra of the PANI, PANI-P1 and PANI-P2 films after solubilization in DMF solutions and figures 4b and 5b show the UV-Vis absorption spectra of P1 and P2 in DMF.

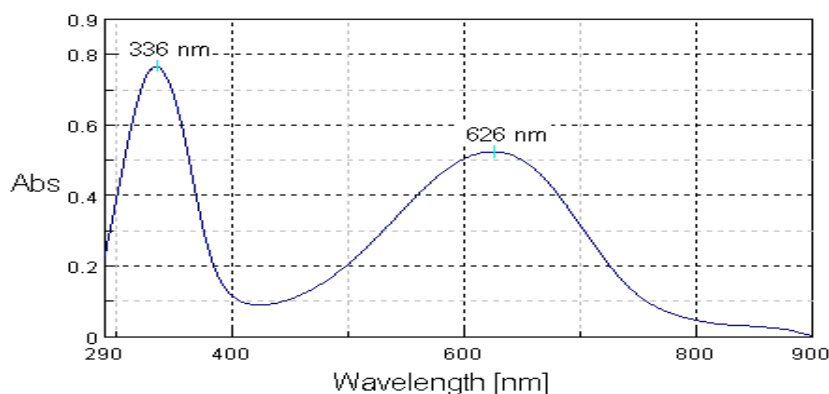


Fig. 3. Absorption spectrum of PANI film dissolved in DMF solution.

A blue solution was obtained upon dissolution in DMF of the green PANI film deposited on the Pt electrode. The various PANI oxidation states have different colors with green corresponding to the emeraldine salt oxidation state and blue being attributed to the emeraldine base state [4]. This implies that in our case the resulted solution contains the emeraldine base oxidation state of PANI.

The shape of the UV-Vis spectrum recorded for this solution corresponds to the shape of the PANI UV-Vis spectra previously reported in the literature [31-33]. According to [33], in case of the emeraldine base oxidation state of PANI, the first absorption maximum can occur at wavelengths as low as 320 nm and is attributed to the π - π^* electronic transition, while the second maximum can be observed at wavelengths slightly over 600 nm and has been attributed to a local charge transfer between a quinoid ring and the adjacent imine-phenyl-amine units. The spectrum presented in figure 3 shows an absorption maximum at 336 nm, probably corresponding to the π - π^* transitions of aniline, while the broad band with a maximum at 626 nm is due to n- π^* transitions of quinone-imine groups.

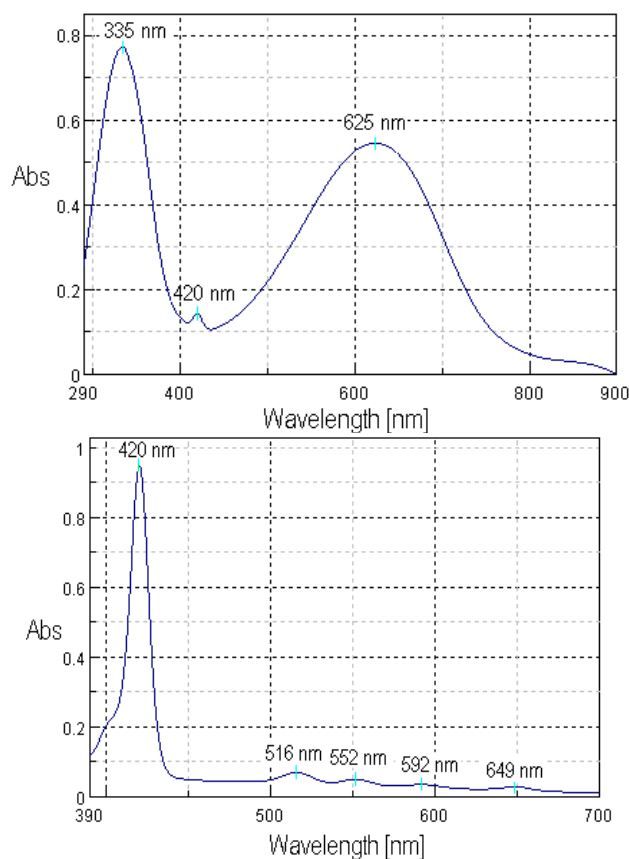


Fig. 4. a) Absorption spectrum of PANI-P1 film solubilized in DMF solution;
b) Absorption spectrum of P1 in DMF solution

The presence of an additional absorption band with a maximum at 420 nm can be observed on the spectrum shown in figure 4a. This maximum appears at exactly the same wavelength as the maximum of the Soret band observed in the P1 spectrum (figure 4b), indicating the presence of this porphyrin in the DMF solution containing the PANI-P1 solubilized film.

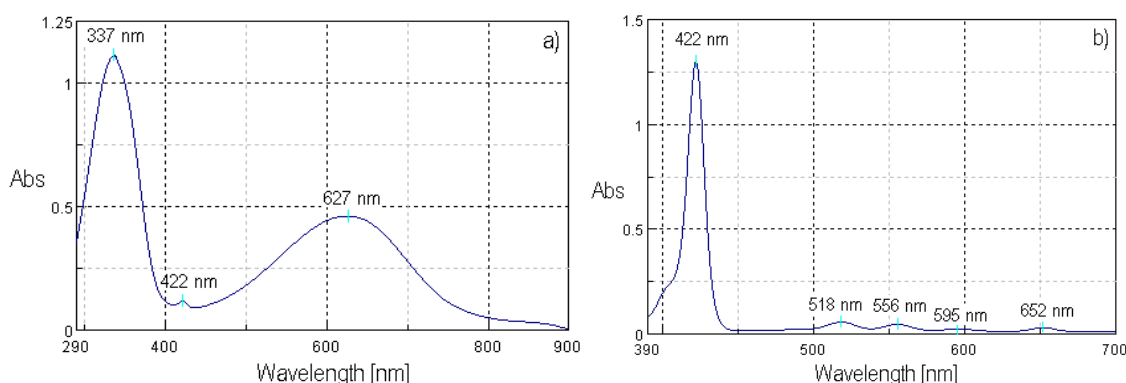


Fig. 5. a) Absorption spectrum of PANI-P2 film solubilized in DMF solution;
b) Absorption spectrum of P2 in DMF solution

The UV-Vis spectrum of the PANI-P2 solubilized film (figure 5a) shows the Soret band of the corresponding P2 porphyrin (figure 5b) at 422 nm. The shape of the spectra recorded for the PANI-P1 and PANI-P2 films show the two PANI characteristic absorption bands at almost identical wavelengths as the ones observed in figure 3.

Electrochemical behavior of PANI, PANI-P1 and PANI-P2 electrodes

The electrochemical behavior of the three types of modified Pt electrodes was investigated by cyclic voltammetry in 0.1 and 0.5 M H_2SO_4 aqueous solutions. Figure 6 shows the overlay of the last aniline polymerization cycle with the first cycles recorded in monomer-free 0.5 M sulfuric acid solution corresponding to the PANI, PANI-P1 and PANI-P2 films.

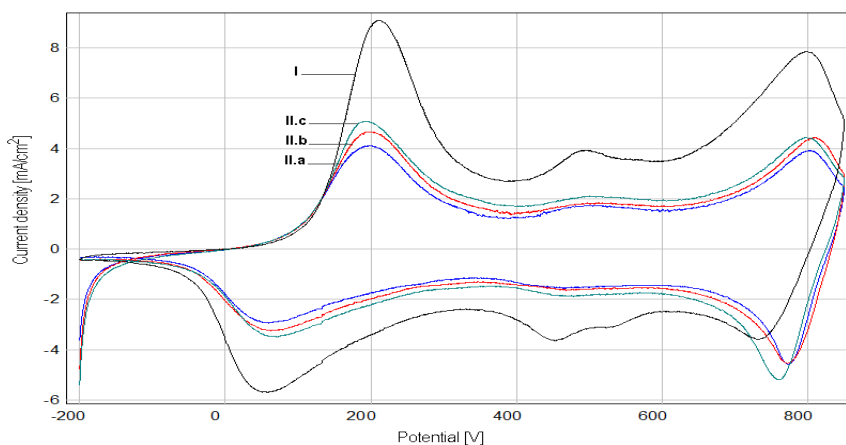


Fig. 6. Comparison between: I. PANI generation process (final cycle); II. Characterization in monomer-free 0.5 M H_2SO_4 solution for the a) PANI, b) PANI-P1 and c) PANI-P2 electrodes (cycle 1). Potential range $-0.2 \div 0.85$ V, $\nu = 0.05$ V s^{-1}

The shapes of the voltammograms recorded for the three modified electrodes in monomer-free acid solution are very similar and show the two pairs of redox processes (**1a-1c** and **2a-2c**) attributed to the interchanging between leucoemeraldine base/emeraldine salt and emeraldine salt/pernigraniline salt, respectively. The processes attributed to secondary products or intermediary compounds are also observable.

The current densities of the anodic and cathodic peaks corresponding to the modified electrodes in monomer-free solution are smaller than those corresponding to the last cycle of the PANI generation process. The only exception can be observed for the cathodic peaks present in the $0.7 \div 0.8$ V range, where the current densities of the modified electrodes are higher. This means

that the reduction process of pernigraniline salt to emeraldine salt is intensified in monomer-free solution, especially in case of the PANI-P2 electrode. With regard to the oxidation and reduction peak potentials, the peaks of the modified electrodes in monomer-free H_2SO_4 solution are slightly shifted, some toward more positive potential values and others toward more negative ones. In case of the pernigraniline salt to emeraldine salt reduction process, a more pronounced shift can be observed toward more positive values and so the process takes place earlier during the reverse scan.

Cyclic voltammograms recorded for the PANI, PANI-P1 and PANI-P2 electrodes, in 0.5 and 0.1 M H_2SO_4 solutions. Figure 7 shows the voltammograms obtained in 0.1 M H_2SO_4 solution.

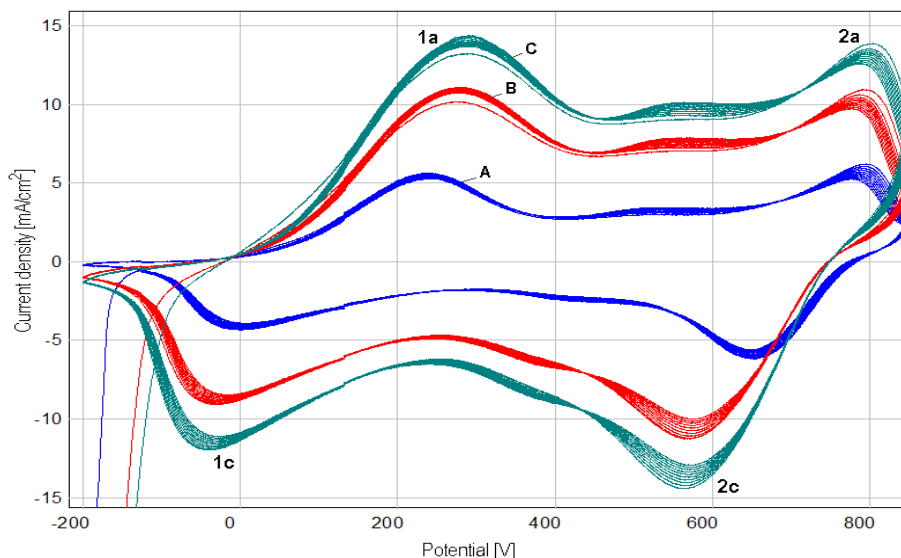


Fig. 7. Cyclic voltammograms of: A) PANI; B) PANI-P1 and C) PANI-P2, recorded in 0.1 M H_2SO_4 solution, potential range: $-0.2 \div 0.85$ V, 10 cycles, $\nu = 0.05$ V s^{-1}

The behavior of the three modified electrodes during the 10 voltammetric scans in monomer-free 0.5 M acid solution is the same in all cases and consists in a decrease of current densities corresponding to the **1a-1c** and **2a-2c** redox processes as the number of recorded cycles increases. The current densities of the remaining peaks increase with the number of cycles, implying that in the absence of aniline, the reactions corresponding to these peaks are intensified.

The shape of the voltammograms recorded for the PANI-P1 and PANI-P2 electrodes are very similar, indicating that the initial PANI film remains distinct. However, current densities observed in the presence of adsorbed porphyrins are higher than those observed for the PANI electrode, evidencing an enhancement of the processes attributed to the redox transitions of PANI.

In monomer-free 0.1 M H_2SO_4 solution, the shape of the voltammograms corresponding to the modified electrodes changes with the number of recorded cycles in the same way as it did in the 0.5 M H_2SO_4 solution. However, in the presence of adsorbed porphyrins on the PANI films, the anodic and cathodic processes are enhanced even more for this solution. As can be seen from table 2, in case of the PANI-P2 electrode, the current density corresponding to the anodic peak (**1a**) attributed to the formation of emeraldine salt is 13.64 mA/cm² in 0.1 M acid solution, while in 0.5 M solution its 5.95 mA/cm². This behavior observed for the porphyrin modified electrodes is interesting and merits further study in solutions with different pH values.

The influence of the scan rate on the PANI, PANI-P1 and PANI-P2 modified electrodes was investigated in 0.5 M H_2SO_4 . For all three modified electrodes, as the value of the scan rate increased the anodic and cathodic current densities increased as well. Scan rate increase also affects the peak potential values, shifting the anodic peaks toward more positive potentials and the cathodic peaks toward more negative potential values.

Table 2. Potential and current density values of peaks corresponding to the **1a-1c** and **2a-2c** redox couples observed for the 10th cycle recorded for the PANI, PANI-P1 and PANI-P2 films in 0.1 M H₂SO₄ solution.

0.1 M H ₂ SO ₄				
Anodic peaks				
1a			2a	
	E(V)	i(mA/cm ²)	E(V)	i(mA/cm ²)
PANI	0.240	5.28	0.777	5.27
PANI-P1	0.277	10.71	0.777	9.73
PANI-P2	0.287	13.64	0.788	12.60
Cathodic peaks				
1c			2c	
	E(V)	i(mA/cm ²)	E(V)	i(mA/cm ²)
PANI	0	-3.93	0.650	-5.60
PANI-P1	-0.015	-8.49	0.575	-10.00
PANI-P2	-0.025	-11.12	0.573	-12.93

The dependence of anodic and cathodic peak currents corresponding to the leucoemeraldine/emeraldine redox couple on the scan rate and the square root of the scan rate was also studied. Figure 8 shows the dependency of these peak currents (*I_p*) on the square root of the scan rate, for the three modified electrodes, as well as the slope and R² values corresponding to the anodic dependencies.

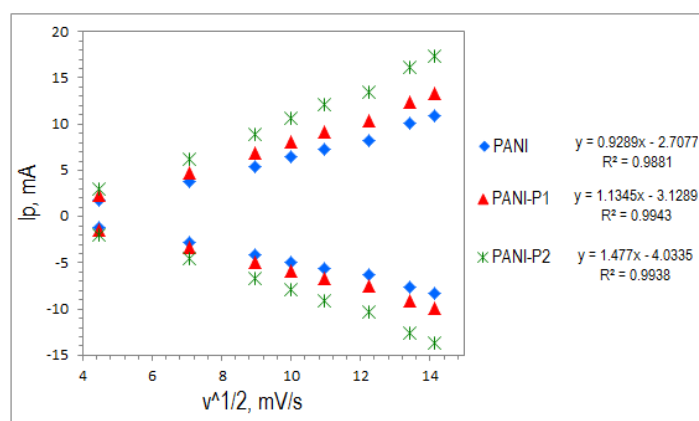


Fig. 8. Anodic and cathodic peak currents corresponding to the first redox process vs. square root of scan rate, for the PANI, PANI-P1 and PANI-P2 electrodes and the line equations of the anodic dependencies.

A high degree of substrate adherence can be attributed to the three films based on the linear relationships obtained from the peak currents vs. scan rate dependency (not shown). The linear relationships of anodic and cathodic peak currents vs. the square root of scan rate implied that the electron transfer process for the three systems under consideration is essentially diffusion-controlled. Since the values of the slopes obtained for the anodic peak current vs. square root of scan rate are directly proportional with the electroactivities of the films [34], we can conclude that the electroactivity of the three films decreases in the order: PANI-P2 > PANI-P1 > PANI.

Determination of the PANI film capacitance with and without adsorbed porphyrins

Curves obtained using cyclic voltammetry can be used to calculate the capacitance of an electrical double layer by selecting a potential range where no faradic currents are present. In case of PANI films, the double layer capacitance at the electrode/electrolyte solution interface is very small in comparison with the capacitance of the oxidized film and can be neglected. Because of this, the capacitance calculated based on voltammetric curves is the capacitance of the oxidized PANI film [35,28].

Cyclic voltammograms were recorded for each type of modified electrode in 0.5 M H₂SO₄ electrolyte solution, at different scan rates, in the potential range 0.3 ÷ 0.45 V (showing no faradic currents). Figure 9 shows the voltammograms recorded for the PANI-P2 modified electrode.

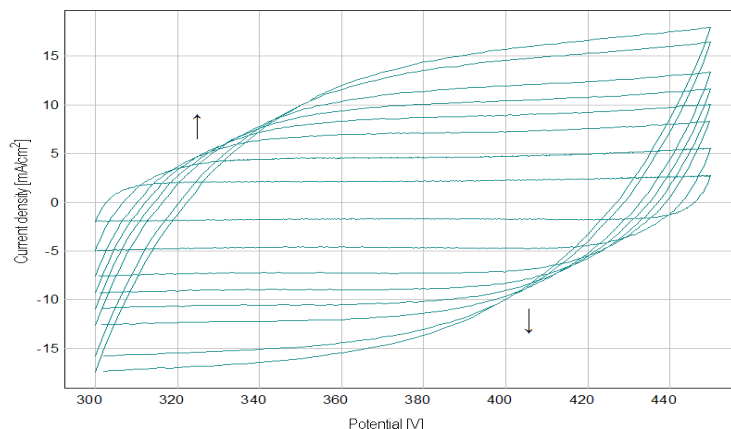


Fig. 9. Cyclic voltammograms of PANI-P2 modified electrode recorded in 0.5 M H₂SO₄ solution, potential range 0.3 ÷ 0.45 V, scan rates: 20, 50, 80, 100, 120, 150, 180, 200 V s⁻¹

As the scan rate value increases, the current density values of the anodic and cathodic branches also increase. For all modified electrodes, the values of the anodic and cathodic capacitive current densities were obtained from the voltammograms recorded for each scan rate and corresponding to the current density values observed at 0.375 V. The mean value of each pair of anodic and cathodic current densities (*idl*) was plotted on the capacitive current density vs. scan rate chart (Figure 10).

The capacitance of the PANI, PANI-P1 and PANI-P2 films was obtained from the slope of the capacitive current density vs. scan rate dependence. The capacitance values of the films were: 6.38 × 10⁻² F cm⁻² for PANI film; 6.52 × 10⁻² F cm⁻² for PANI-P1 and 6.64 × 10⁻² F cm⁻² for the PANI-P2 film. This difference in capacitance between the three types of films is very small, implying that the influence of the porphyrin absorption process on film capacitance is negligible. Since there is a known direct dependency between a film's thickness and its capacitance [28], it is safe to assume that the modification of PANI film thickness due to porphyrin absorption is also very small.

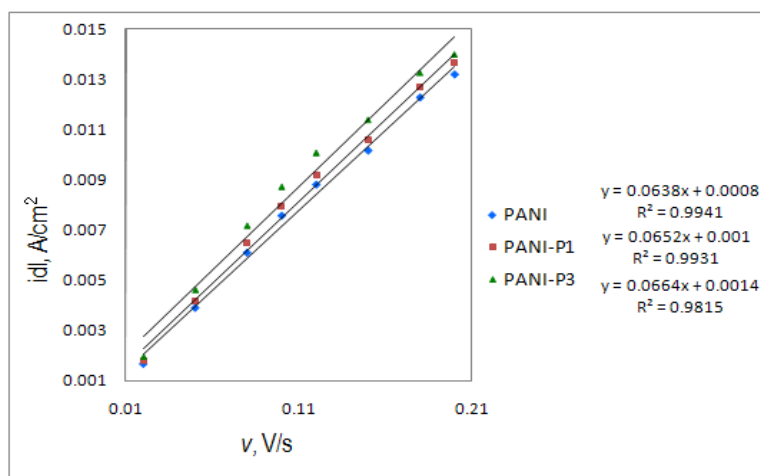


Fig. 10. Dependence of the capacitive current density on scan rate for the PANI, PANI-P1 and PANI-P2 modified electrodes

Potentiometric measurements

The potentiometric properties of the PANI, PANI-P1 and PANI-P2 modified electrodes were investigated in several separate aqueous test solutions containing Ag^+ , Cu^{2+} , Cr^{3+} , Ca^{2+} , Co^{2+} , Na^+ , Al^{3+} , Mg^{2+} , Zn^{2+} , Cd^{2+} , Pb^{2+} , Sr^{2+} , Ba^{2+} , Ni^{2+} and K^+ . Absorption of porphyrin on PANI is justified by the purpose of achieving uniform ionophore deposition and of preventing further H and J aggregation phenomena in acid media. Evaluation of potentiometric response for the three types of electrodes in the presence of cations was performed in the concentration range $10^{-1} \div 10^{-5}$ M. Potentiometric calibration curves were obtained based on measurement values. Figure 11 shows the responses of the modified electrodes toward solutions containing Ag^+ , Cu^{2+} , Cr^{3+} , Ca^{2+} and Al^{3+} cations.

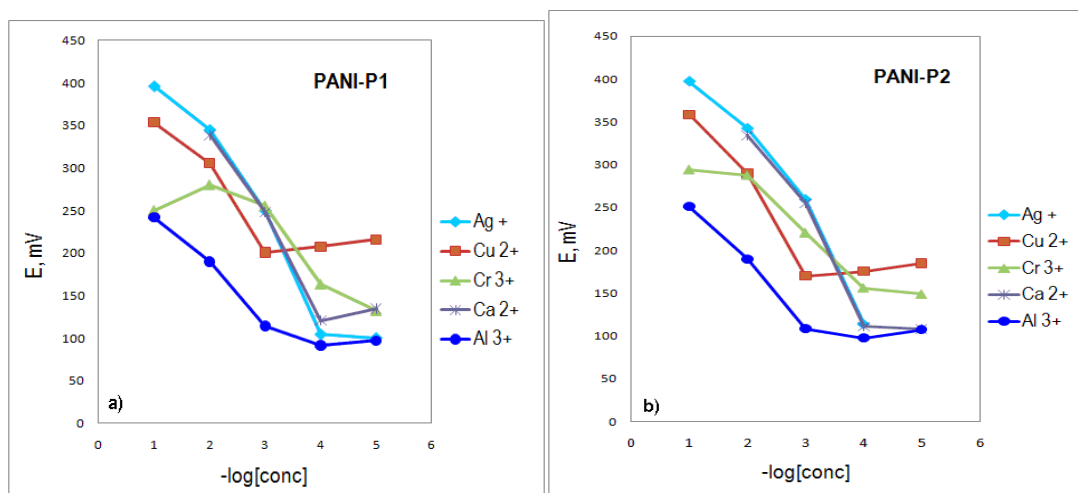


Fig. 11. Potentiometric responses of the PANI-P1 and PANI-P2 electrodes in separate aqueous test solutions containing Ag^+ , Cu^{2+} , Cr^{3+} , Ca^{2+} and Al^{3+} cations, in the $10^{-1} \div 10^{-5}$ M concentration range.

For Ag^+ , the responses obtained for the PANI-P1 and PANI-P2 electrodes in the range $10^{-1} \div 10^{-5}$ M encourage us to continue investigating these sensing materials. In a narrower concentration range ($10^{-2} \div 10^{-5}$ M), Ca^{2+} is interfering with the Ag^+ determination. Based on these preliminary results it can be concluded that in the presence of porphyrins the PANI-P1 and PANI-P2 electrodes

might be suitable for Ag^+ detection, especially since cations such as Cu^{2+} , Cr^{3+} and Al^{3+} don't interfere with its determination.

4. Conclusions

In the present work we described a comparative study between PANI modified platinum electrodes in the presence and absence of two types of porphyrins adsorbed on their surface.

UV-Vis spectroscopy studies performed on the solubilized PANI-P1 and PANI-P2 films confirmed the presence of the Soret band of porphyrins together with the PANI characteristic absorption bands.

Voltammograms recorded in monomer free 0.1 and 0.5 M H_2SO_4 solutions revealed that the three types of investigated electrodes had very similar shapes and that the current densities of peaks corresponding to the leucoemeraldine base/emeraldine salt and emeraldine salt/permanganine salt reversible transitions decrease with the number of recorded cycles. The presence of adsorbed porphyrins enhanced the electrode reactions attributed to the redox transitions of PANI by increasing the corresponding current densities, especially in the case of P2. The linear relationship of anodic and cathodic peak currents vs. scan rate and square root of scan rate showed an increase in film electroactivity for the modified electrodes, described by the sequence: PANI-P2 > PANI-P1 > PANI.

The difference in capacitance values determined by cyclic voltammetry for the investigated films was very small: $6.38 \times 10^{-2} \text{ F cm}^{-2}$ for PANI; $6.52 \times 10^{-2} \text{ F cm}^{-2}$ for PANI-P1 and $6.64 \times 10^{-2} \text{ F cm}^{-2}$ for PANI-P2. This implied that the influence of the porphyrin absorption process on capacitance and film thickness was negligible.

The potentiometric evaluation of PANI films with free-base porphyrins adsorbed on their surface towards several cations revealed super Nernstian responses. Based on these preliminary results it can be concluded that in the presence of porphyrins the PANI-P1 and PANI-P2 electrodes might be suitable for Ag^+ detection, especially since cations such as Cu^{2+} , Cr^{3+} and Al^{3+} don't interfere with its determination. We intend to improve the sensing characteristics of these modified electrodes.

Acknowledgements.

This paper was partially supported by Institute of Chemistry Timisoara of Romanian Academy Programme 2/2014 and Project STAR-SAFEAIR/76/2013.

References

- [1] N. Plesu, A. Kellenberger, I. Taranu, B.O. Taranu, I. Popa, *React. Funct. Polym.* **73**, 772 (2013).
- [2] M. J. Winokur, Chapter 25: *Structural Studies of Conducting Polymers*, in: T.A. Skotheim et al. (Ed.), *Handbook of Conducting Polymers*, 2nd ed., Marcel Dekker Inc., New York, 707-726 (1998).
- [3] D. Schaming, A. Giraudeau, L. Ruhlmann, Chapter 3: *Oxidation of Porphyrins in the Presence of Nucleophiles: From the Synthesis of Multisubstituted Porphyrins to the Electropolymerization of the Macrocycles*, in E. Schab-Balcerzak (Ed.), *Electropolymerization*, InTech, Rijeka, Croatia, 53-76 (2011).
- [4] M.M. Gvozdencovic, B.Z. Jugovic, J.S. Stevanovic, T.L. Trisovic and B.N. Grgur, Chapter 4: *Electrochemical Polymerization of Aniline*, in: E. Schab-Balcerzak (Ed.), *Electropolymerization*, InTech, Rijeka, Croatia, 77-96 (2011).
- [5] S. Pruneanu, E. Veress, I. Marian, L. Oniciu, *J. Mater. Sci.*, **34**, 2733 (1999).
- [6] O. Korostynska, K. Arshak, E. Gill, A. Arshak, *Sensors*, **7**, 3027 (2007).
- [7] G.A. Evtugyn, R.V. Shamagsumova, E.E. Stoikova, R.R. Sitdikov, I.I. Stoikov,

- H.C. Budnikov, A.N. Ivanov, I.S. Antipin, *Electroanal.*, **23**(5), 1081 (2011).
- [8] E. Făgădar-Cosma, D. Vlascici G. Făgădar-Cosma, *Porphyrins from Synthesis to Applications*, Eurostampa, Timișoara, Romania, 10-95 (2008).
- [9] O. Vakuliuk, F.G. Mutti, M. Lara, D.T Gryko., W. Kroutil, *Tetrahedron Lett.*, **52**(28), 3555 (2011).
- [10] A. Molinari, A. Maldotti, A. Bratovcic, G. Magnacca, *Catal. Today*, **161**, 64 (2011).
- [11] H.M. Wang, J.Q. Jiang, J.H. Xiao, R.L. Gao, F.Y. Lin, X.Y. Liu, *Chem. Biol. Interact.*, **172**, 154 (2008).
- [12] C.-W. Lee, H.-P. Lu, N.M. Reddy, H.-W. Lee, E. W.-G. Diau, C.-Y. Yeh, *Dyes Pigments*, **91**, 317 (2011).
- [13] Q. Tan, X. Zhang, L. Mao, G. Xin, S. Zhang, *J. Mol. Struct.*, **1035**, 400 (2013).
- [14] Y.I. Kuznetsov, *Int. J. Corros. Scale Inhib.*, **1**(1), 3 (2012).
- [15] J.S. Woods, M.D. Martin, B.G. Leroux, T.A. DeRouen, M.F. Bernardo, H.S. Luis, J.G. Leitao, P.L. Simmonds, T.C. Rue, *Clin. Chim. ACTA*, **405**, 104 (2009).
- [16] J. Kim, S.-H. Lim, Y. Yoon, T.D. Thangadurai, S. Yoon, *Tetrahedron Lett.*, **52**, 2645 (2011).
- [17] D. Vlascici, I. Popa, V.A. Chiriac, G. Fagadar-Cosma, H. Popovici, E. Fagadar-Cosma, *Chem. Cent. J.*, **7**:111 (2013).
- [18] R. Cristescu, C. Popescu, A.C. Popescu, S. Grigorescu, I.N. Mihailescu, A.A. Ciucu, S. Iordache, A. Andronie, I. Stamatina, E. Fagadar-Cosma, D.B. Chrisey, *Appl. Surf. Sci.*, **257**(12), 5293 (2011).
- [19] M. Popescu, I.D. Simandan., F. Sava, A. Velea, E. Fagadar-Cosma, *Digest Journal of Nanomaterials and Biostructures*, **6**(3), 1253 (2011).
- [20] E. Fagadar-Cosma, L. Cseh, V. Badea, G. Fagadar-Cosma, D. Vlascici, *Comb. Chem. High T. Scr.*, **10**, 466 (2007).
- [21] S. Grama, N. Hurduc, E. Fagadar-Cosma, M. Vasile, E. Tarabukina, G. Fagadar-Cosma, *Dig. J. Nanomater.Bios.*, **5**, 959 (2010).
- [22] L. Lvova, R. Paolesse, C. Di Natale, A. D'Amico, A. Bergamini, *Int. J. Electrochem.*, **2011**, 1 (2011).
- [23] E. Fagadar-Cosma, G. Fagadar-Cosma, M. Vasile, C. Enache, *Curr. Org. Chem.*, **16**(24), 931 (2012).
- [24] Z. Dudas, C. Enache, G. Fagadar-Cosma, I. Armeanu, E. Fagadar-Cosma, *Mater. Res. Bull.*, **45**, 1150 (2010).
- [25] J. S. Lindsey, H. C. Hsu, I. C. Schreiman, *Tetrahedron Lett.*, **27**(41), 4969 (1986).
- [26] V. Sol, V. Chaleix, R. Granet, P. Krausz, *Tetrahedron*, **64**, 364 (2008).
- [27] Y. Atassi, M. Tally, *Electrochemical Polymerization of Anilinium hydrochloride*, e-print arXiv:1307.5668, 1 (2013).
- [28] N. Plesu, A. Kellenberger, M. Mihali, N. Vaszilcsin, *J. Non-Cryst. Solids*, **356**, 1081 (2010).
- [29] B. Silwana, C. van der Horst, E. Iwuoha, V. Somerset, Chapter 5: *Inhibitive Determination of Metal Ions Using a Horseradish Peroxidase Amperometric Biosensor*, in: T. Rinken (Ed.), *State of the Art in Biosensors - Environmental and Medical Applications*, InTech, Rijeka, Croatia, 105-119 (2013).
- [30] S. Tawde, D. Mukesh, J.V. Yakhmi, *Synthetic Metals*, **125**, 401 (2002).
- [31] I. Venditti, I. Fratoddi, M.V. Russo, A. Bearzotti., *Nanotechnology*, **24**(15), 155503 (2013).
- [32] C. Yang, Z. Fang, P. Zhang, *J. Cent. South Univ. Technol.*, **6**(2), 127 (1999).
- [33] R. Singh, *Chlorophyll-a Titanium Dioxide Donor-Acceptor System - in Conducting Polyaniline Grana-Like Matrix*, Thesis submitted for Masters of Technology in Nanoscience & Technology degree, 13-14 (2013).
- [34] A. Arslan, E. Hur, *Int. J. Electrochem. Sci.*, **7**, 12558 (2012).
- [35] G. Sandi, P. Vanysek, *Synth. Met.*, **64**, 1 (1994).